Electronic Supplementary Material (ESI) for Energy & Environmental Science.

*Electronic Supplementary Information (ESI) for:*

# *Microkinetic Model for pH- and Potential-Dependent Oxygen Evolution during Water Splitting on Fe-Doped $\beta$-NiOOH*

*Ananth Govind Rajan*[1,2] *and Emily A. Carter*[1,3,4]*

[1] Department of Mechanical and Aerospace Engineering, Princeton University, Princeton, New Jersey 08544-5263, United States

[2] Present address: Department of Chemical Engineering, Indian Institute of Science, Bengaluru, Karnataka 560012, India

[3] Department of Chemical and Biomolecular Engineering, University of California, Los Angeles, Los Angeles, California 90095-1592, United States

[4] Office of the Chancellor, Box 951405, University of California, Los Angeles, Los Angeles, California 90095-1405, United States

***Corresponding Author:** Emily A. Carter (E-mail: eac@princeton.edu and eac@ucla.edu)

**Table of Contents**

## S1. Equivalence of the OER reduction potentials for $H^+$- and $OH^-$-based pathways

The oxygen evolution reaction (OER) can be written via protons in solution as:

$$2H_2O \rightarrow O_2 + 4(H^+ + e^-) \tag{A}$$

and via hydroxide ions in solution as:

$$4OH^- \rightarrow O_2 + 2H_2O + 4e^- \tag{B}$$

The pH dependence of any reaction's reduction potential can be modeled through the Nernst equation:

$$E_{red} = E_{red}^0 - \frac{0.059}{n} \log Q_{red} \tag{S1}$$

where the above equation is written for room temperature, $E_{red}$ is the reduction potential, $E_{red}^0$ is the standard reduction potential, $n$ is the number of electrons participating in the reaction, and $Q_{red}$ is the reaction quotient. Since we are considering reduction potentials, we will be working with the reverse reactions of (A) and (B). We will initially use the standard hydrogen electrode (SHE) as the reference electrode, and will later extend the result to the reversible hydrogen electrode (RHE).

For reverse reaction (A), i.e., $O_2 + 4(H^+ + e^-) \rightarrow 2H_2O$, $E_{red}^0$ = 1.23 V versus the SHE and $n$ = 4, such that the Nernst equation can be written as:

$$E_{red} = 1.23 - \frac{0.059}{4} \log\left(\frac{a_{H_2O}^2}{a_{O_2} a_{H^+}^4}\right) \tag{S2}$$

where $a_i$ denotes the activity of the $i^{\text{th}}$ species involved in the reaction. Now, for pure water ($a_{H_2O}$ = 1), $O_2$ gas at 1 bar pressure ($a_{O_2}$ = 1), and $a_{H^+} = 10^{-\text{pH}}$, we have:

$$E_{red} = 1.23 - 0.059pH \tag{S3}$$

For reverse reaction (B), i.e., $O_2 + 2H_2O + 4e^- \rightarrow 4OH^-$, $E_{red}^0$ = 0.40 V versus the SHE and $n$ = 4, such that the Nernst equation can be written as:

$$E_{red} = 0.40 - \frac{0.059}{4} \log\left(\frac{a_{OH^-}^4}{a_{H_2O}^2 a_{O_2}}\right) \tag{S4}$$

For pure water ($a_{H_2O}$ = 1), $O_2$ gas at 1 bar pressure ($a_{O_2}$ = 1), and $a_{OH^-} = 10^{-(14-\text{pH})}$, we have:

$$E_{red} = \; = 0.40 + 0.059(14 - pH) = 1.23 - 0.059pH \tag{S5}$$

Thus, we have demonstrated, using Eqs. (S3) and (S5), that the OER reduction potential does not depend on whether the reaction is balanced via $H^+$ or $OH^-$. Although we have assumed pure water and $O_2$ at 1 bar pressure, the above analysis can be carried out for any arbitrary values of the water and oxygen activities, still showing the OER reduction potentials via protons and hydroxide ions to be equal. Nevertheless, for use in the Marcus theory equation, one needs the *standard* (unit activity) reduction potentials, i.e., for reactions through $H^+$ (pH=0), 1.23 V, and for reactions through $OH^-$ (pH=14), 0.40 V, versus the standard hydrogen electrode (SHE).

Instead of the pH-independent SHE, one could also use the pH-dependent reversible hydrogen electrode (RHE) as a reference. At room temperature, the potential of the RHE is given as: $E_{RHE} = -0.059pH$. Accordingly, if the RHE is used as a reference, the reduction potentials of the OER via $H^+$ or $OH^-$ would both be equal to:

$$\begin{aligned} E_{red,RHE} &= E_{red,SHE} - E_{RHE} \\ &= E_{red,SHE} + 0.059pH \\ &= 1.23\text{ V} \end{aligned} \tag{S6}$$

for any pH considered at room temperature. As a result, the *standard* reduction potential for both reactions via $H^+$ (pH=0) and $OH^-$ (pH=14) would also be 1.23 V.

## S2. Why do we use the solubility of oxygen in pure water, rather than in aqueous KOH, in our model?

In the microkinetic model presented in the main text, we used the solubility of oxygen in pure water, rather than in aqueous KOH, for calculating the oxygen activity. To demonstrate that this assumption is well founded, we re-calculated the OER current density from our microkinetic model using oxygen solubility in an appropriate concentration of KOH, as opposed to that in pure water. We used the correlation for oxygen solubility in aqueous KOH at 25 °C presented in Davis et al.: $\log_{10} S = \log_{10}(1.26 \times 10^{-3}) - 0.1746C$, where $S$ is the oxygen solubility in mol/L and $C$ is the KOH concentration, also in mol/L.[1]

The new results are summarized in Figure S1 and consider four different cases: best-fit parameters obtained using oxygen solubility in pure water (i, ii) and in aqueous KOH (iii, iv). The predictions are made using the oxygen solubility in water in cases (i)/(iii) and using the oxygen solubility in aqueous KOH in cases (ii)/(iv). The results indicate that, using the best-fit parameters derived by fitting our model with oxygen solubility in pure water (as done in the main text), the RMSD of the predicted data increases from 0.26 in case (i) to 0.30 in case (ii), where oxygen is assumed to be dissolved in pure water in the former (Figure S1A) as opposed to in aqueous KOH in the latter (Figure S1B). This indicates that the medium in which oxygen is assumed to be dissolved does not affect the OER current density significantly, under the conditions we have considered. One can also infer from panels A and B of Figure S1, that the model compares favorably to the experimental data in both the scenarios. Similar conclusions are drawn by examining Figure S1C and S1D, which assume oxygen solubility in water and aqueous KOH, respectively, but use the latter assumption to derive the best-fit model parameters.

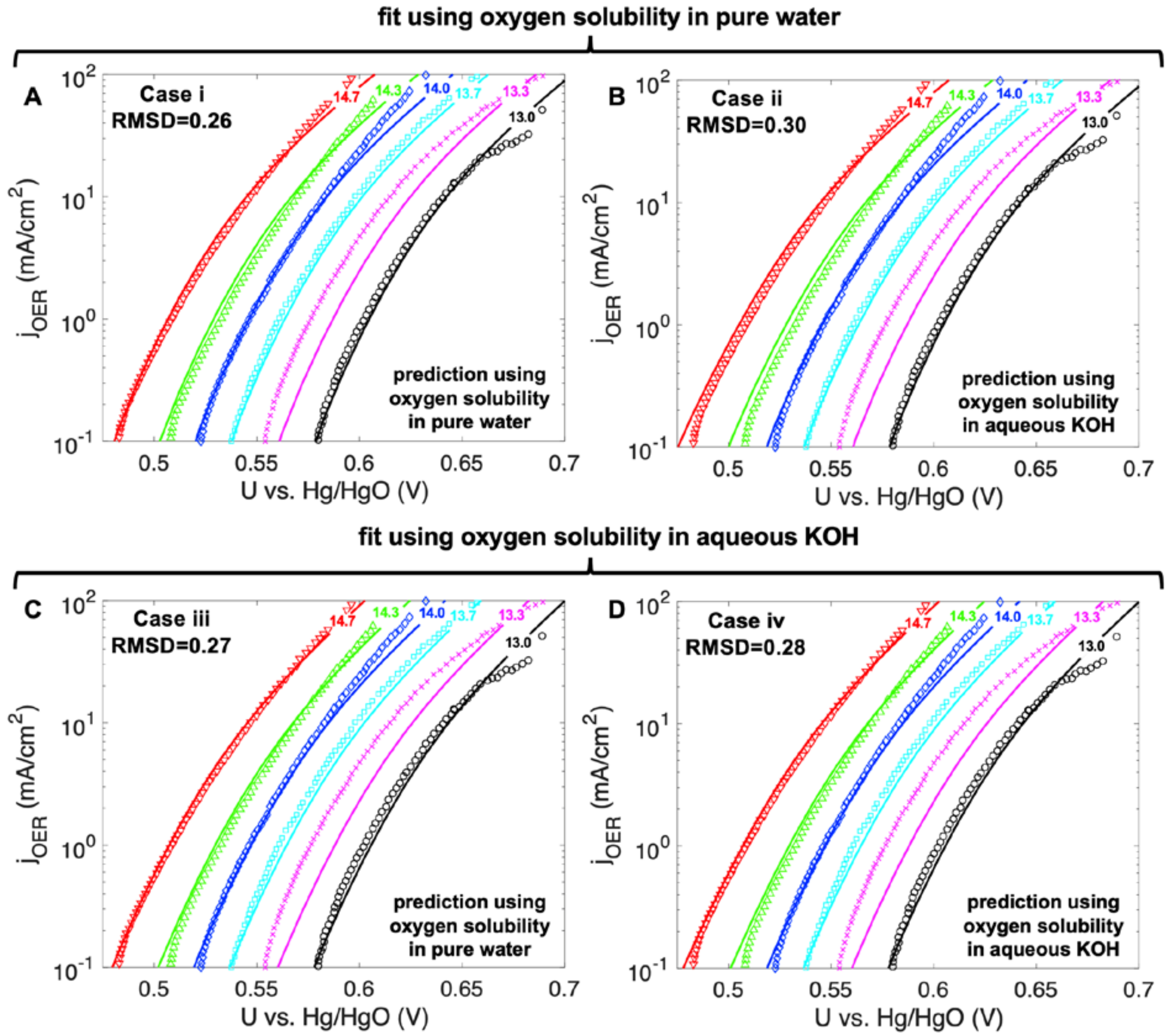

**Figure S1.** Comparison of the predicted and the measured polarization curves (i.e., OER current-density vs. applied-potential plots) for the microkinetic model in four different cases: (A) fit and prediction both using oxygen solubility in pure water, (B) fit and prediction using oxygen solubility in pure water and aqueous KOH, respectively, (C) fit and prediction using the oxygen solubility in aqueous KOH and pure water, respectively, and (D) fit and prediction both using oxygen solubility in aqueous KOH. Experimental data at various pH values are shown using different symbols (13.0 – circles, 13.3 – crosses, 13.7 – squares, 14.0 – diamonds, 14.3 – upward triangles, and 14.7 – downward triangles) and is adapted from the study by Louie and Bell.[2]

Furthermore, we calculated the best-fit parameters for the case when oxygen solubility in aqueous KOH is considered. As seen in Table S1, the ensuing best-fit parameters are qualitatively similar to the best-fit parameters when oxygen solubility in pure water is considered. From a quantitative perspective, the parameter values in the two cases are within the confidence intervals that we predict. Moreover, we calculated the OER current density, at a pH of 14.0 and an applied potential of 0.28 V versus the Hg/HgO electrode, in cases (i) and (iv), respectively, to be 11.1 mA/cm$^2$ and

10.6 mA/cm$^2$, indicating not much difference between the predicted OER current densities, when the respective best-fit parameters are utilized.

**Table S1.** Comparison of the best-fit parameters when the microkinetic model is fit using the oxygen solubility in pure water (second column) and in aqueous KOH (third column). The RMSD values in the two cases also are indicated.

| **Parameter** | **Value when model is fit with oxygen solubility in pure water (eV)** <br> **RMSD (Case i) = 0.26** | **Value when model is fit with oxygen solubility in aqueous KOH (eV)** <br> **RMSD (Case iv) = 0.28** |
|---|---|---|
| $\boldsymbol{w_{ions}}$ | $0.607 \pm 0.054$ | $0.650 \pm 0.017$ |
| $\boldsymbol{w_{water}}$ | $0.065 \pm 0.017$ | $0.010 \pm 0.042$ |
| $\boldsymbol{\lambda_{H^+}}$ | $0.744 \pm 0.219$ | $0.583 \pm 0.134$ |
| $\boldsymbol{\lambda_{OH^-}}$ | $2.474 \pm 0.174$ | $2.595 \pm 0.072$ |

Finally, there is a distinct advantage of considering oxygen solubility in water, rather than in KOH, for our model. Namely, the oxygen solubility data in Davis et al.[1] are only for three different temperatures (0 °C, 25 °C, and 60 °C), thereby acting as an impediment to predicting the OER current density under arbitrary electrolyzer operating conditions. This means that, assuming oxygen to be dissolved in pure water, as opposed to in aqueous KOH, while parametrizing the microkinetic model, not only does not compromise on model accuracy but also allows the model to be versatile by allowing for kinetic predictions at any desired temperature.

## S3. Why is it essential to use the reversible hydrogen electrode as a reference in the proposed microkinetic model?

As mentioned in the main text, we found that it is essential to use the reversible hydrogen electrode (RHE) as a reference in the microkinetic model, in order to obtain good agreement of the model with experimental polarization curves. Why is this so? We showed in Section S1 above that the OER has equal reduction potentials at a given pH whether it is balanced by $H^+$ or $OH^-$. However, we also saw in Section S1 that the *standard* OER reduction potential is 1.23 V when balanced by $H^+$ (i.e., at pH=0) and 0.40 V when balanced by $OH^-$ (i.e., at pH=14). This dichotomy, i.e., equal reduction potentials, but unequal *standard* reduction potentials occurs because we use different pHs as the standard states for the reactions via $H^+$ and $OH^-$. The choice of different standard pHs is understandable because one defines the respective standard state based on the corresponding ion having unit molar concentration. However, this choice causes the reactions via $H^+$ and $OH^-$ to be treated differently when the SHE is used as a reference electrode, even though thermodynamics dictates that their reduction potentials should be equivalent. Instead, when the RHE is used as a reference using the respective standard pHs (see Eq. (26) in the main text), i.e., $pH^0 = 0$ for the reactions via $H^+$ and $pH^0 = 14$ for the reactions via $OH^-$, the standard reduction potentials become equal for reactions via $H^+$ and $OH^-$ (see, e.g., Figure 1B and Table 1 in the main text and Section S1 in the ESI). However, still the active pH needs to be used as the reference state for the applied potential, as done in Eq. (25) of the main text. The choice of the standard pHs and active pH in the RHE for the standard states and active state, respectively, is consistent with the RHE's working principle that its pH is identical to the pH of the solution, in which the electrode, against which it is used as a reference, is immersed.

To conclusively rule out the use of pH-independent reference electrodes (e.g., the SHE), we carried out a fit of the microkinetic model to experimental data from Louie and Bell,[2] using the SHE as a reference electrode. Figure S2A shows a comparison of the measured and fitted OER polarization curves. Further, Table S2 lists the best-fit parameters and their 90% confidence intervals (in percent). A comparison of Figure S2A and Figure 4 in the main text indicates that the fit is worse when the SHE is used as a reference electrode. Indeed, we obtain a RMSD of 0.34, as mentioned in Table S2, as compared to a RMSD of 0.26 obtained in the main text. Moreover, an examination of Table S2 tells us that the best-fit parameters obtained using the SHE as a reference electrode are unphysical. For example, the water work term is significantly larger in absolute magnitude than the ionic water term, despite water being a dipole, which would incur less work than an ion, a monopole, in being transported to the surface from the bulk solution. Moreover, the ionic work term is close to zero, indicating the surface does not carry any charge under the highly oxidizing conditions of the OER, an unlikely possibility. In Figure S2B, we plot the OER current densities through $H^+$- and $OH^-$-mediated pathways under various solution pHs and applied potentials. We find that, when the SHE is used as a reference electrode, the microkinetic model predicts highly negative current density values via the $OH^-$-mediated OER pathway. This is an unphysical prediction of the microkinetic model when using the SHE as a reference electrode, as it is unlikely that hydroxide oxidation proceeds in the reverse direction under the highly oxidizing conditions of the OER. In conclusion, we have not only physically rationalized why the RHE is a more appropriate reference electrode for a microkinetic model involving reactions via both $H^+$ and $OH^-$, but also have provided conclusive proof that using the SHE as a reference electrode in the microkinetic model leads to a poorer fit and unphysical predictions/parameter values.

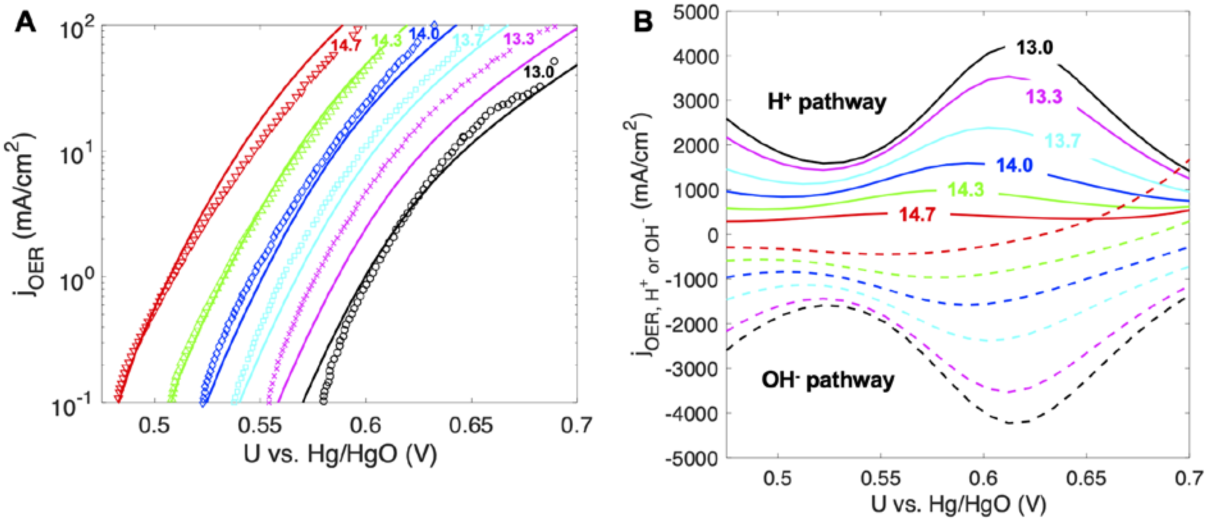

**Figure S2.** (A) Comparison of the fitted and the measured polarization curves (i.e., OER current density vs. applied potential plots) for the microkinetic model using the SHE as the reference for the applied and the standard reaction (reduction) potentials. Experimental data at various pH values are shown using different symbols (13.0 – circles, 13.3 – crosses, 13.7 – squares, 14.0 – diamonds, 14.3 – upward triangles, and 14.7 – downward triangles) and is adapted from the study by Louie and Bell.[2] (B) OER current densities attributed to $H^+$ (solid lines) and $OH^-$ (dashed lines) pathways at various applied potential and pH values using the SHE as the reference electrode in the microkinetic model.

**Table S2.** Fit RMSD, parameters, and the latter's 90% confidence intervals (in percent) when the SHE is used as the reference electrode in the microkinetic model.

| Parameter (RMSD=0.34) | Value (eV) | Percent 90% c.i. |
|---|---|---|
| $\boldsymbol{w_{ions}}$ | -0.005 | 352 |
| $\boldsymbol{w_{water}}$ | -0.504 | 5 |
| $\boldsymbol{\lambda_{H^+}}$ | 0.541 | 8 |
| $\boldsymbol{\lambda_{OH^-}}$ | 1.181 | 2 |

## S4. A plausible explanation for the predicted and measured OER polarization curves not agreeing as well for pH=13.3

We noted in the main text that the agreement between the predicted and measured OER polarization curves is good for all pHs except 13.3. We briefly mentioned there that the agreement is much better if the experimental pH is assumed to be 13.4 or 13.5. Accordingly, Figure S3 depicts the comparison of the predicted and measured current-density versus applied-potential plots, assuming the measured pH of 13.3 to be instead 13.4 (panel A) or 13.5 (panel B), without changing the model parameter values from their respective best-fit ones reported in the main text. It is evident that the predicted and measured curves compare very favorably when such an assumption is made, leading to lower RMSD values of 0.201 and 0.195, respectively, instead of 0.26 as reported using the data presented by Louie and Bell.[2] It follows that a small error (~0.1-0.2) in the measurement of the pH while obtaining the polarization curves could explain the poorer fit seen in Figure 4 of the main text for pH=13.3.

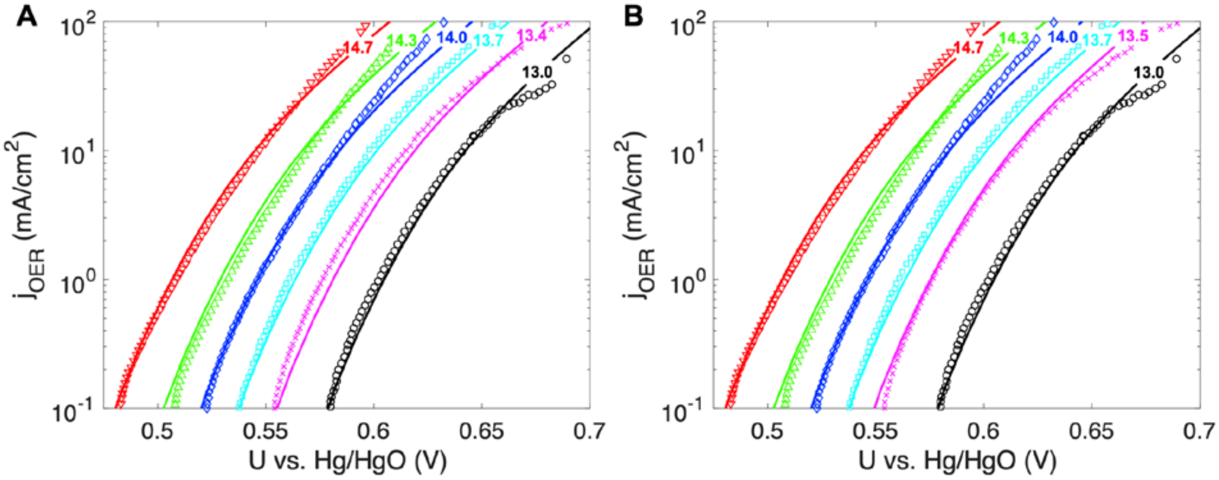

**Figure S3.** Comparison of the predicted and the measured polarization curves (i.e., OER current-density vs. applied-potential plots) assuming pH=13.3 to be 13.4 (A) or 13.5 (B). Experimental data at various pH values are shown using different symbols (13.0 – circles, 13.3 (assumed to be

13.4 in panel A and 13.5 in panel B) – crosses, 13.7 – squares, 14.0 – diamonds, 14.3 – upward triangles, and 14.7 – downward triangles) and is adapted from the study by Louie and Bell.[2]

## S5. Why does the proposed microkinetic model have only four fitting parameters?

To evaluate the robustness of our microkinetic model, we carried out the fitting process multiple times by varying the number of parameters considered, and examining their resultant best-fit values and confidence intervals. We explored four different cases (i)–(iv) below, including the one considered in the main text (case (i)). The following are the additional parameters introduced in cases (ii)–(iv):

- In case (ii) with *five* fitting parameters, we considered $w_{H^+}$ and $w_{OH^-}$ separately, instead of considering $w_{ions}$ as done in the main text.
- In case (iii) with *ten* fitting parameters, we considered separate reorganization free energies for each of the eight reactions in the mechanism, along with $w_{ions}$ for the work term for $H^+$/$OH^-$ ions.
- In case (iv) with *eleven* fitting parameters, we not only considered separate reorganization free energies for each of the eight reactions in the mechanism, but also $w_{H^+}$ and $w_{OH^-}$ separately.

In cases (ii)–(iv), the initial guesses and lower/upper bounds for the parameters were adapted from the respective best-fit parameters and bounds in case (i). Specifically, the initial guess for both $w_{H^+}$ and $w_{OH^-}$ in cases (ii) and (iv) was simply the best-fit $w_{ions}$ value from case (i). Similarly, the initial guesses for $\lambda_{H^+,i}$ and $\lambda_{OH^-,i}$ were the best-fit values of $\lambda_{H^+}$ and $\lambda_{OH^-}$ from case (i). The lower and upper bounds for the work terms were -2 eV and +2 eV, respectively; they were 0 eV and 3 eV for the reorganization free energies.

The fit root-mean-squared deviation (RMSD) and the fit parameters and their 90% confidence intervals (c.i.) are summarized in Tables S3 through S6 below, for cases (i)–(iv), respectively. An examination of the data in Tables S3 through S6 reveals the following observations:

- The RMSD marginally improves with an increase in the number of fitting parameters, because of a greater degree of freedom in parametrizing the model.
- The c.i.'s for the fit parameters increase substantially upon increasing the number of parameters in the model.
- In some cases, increased number of parameters also leads to unphysical parameter values. For example, in case (iii) and (iv), one obtains a negative work term for water, which is unphysical as explained in the main text.
- In cases (iii)–(iv), the reorganization free energy for each reaction via $H^+$ is lower than the that value for the corresponding reaction via $OH^-$. As a result, the conclusion that $\lambda_{H^+} < \lambda_{OH^-}$, made in the main manuscript, is robust.

Based on the above observations, we conclude that the use of four fitting parameters, as done in the main manuscript, not only provides physically relevant parameter values with reasonable confidence intervals, but also leads to a robust conclusion regarding the reorganization free energies, $\lambda_{OH^-} > \lambda_{H^+}$, that is unaltered using a higher number of model parameters.

**Table S3.** Fit RMSD, parameters, and the latter's 90% confidence intervals (in percent) for the *case with four fitting parameters:* two reorganization free energies, one each for $H^+$- and $OH^-$-based reactions, and two work terms, one each for transporting water and ions to the surface; this case is considered in the main text.

| Parameter (RMSD=0.26) | Value (eV) | Percent 90% c.i. |
|---|---|---|
| $w_{ions}$ | 0.607 | 9 |
| $w_{water}$ | 0.065 | 26 |
| $\lambda_{H^+}$ | 0.744 | 29 |
| $\lambda_{OH^-}$ | 2.474 | 7 |

**Table S4** Fit RMSD, parameters, and the latter's 90% confidence intervals (in percent) for the *case with five fitting parameters:* two reorganization free energies, one each for $H^+$- and $OH^-$-based reactions, and three work terms, one each for transporting water, $H^+$, and $OH^-$ to the surface.

| Parameter (RMSD=0.26) | Value (eV) | Percent 90% c.i. |
|---|---|---|
| $w_{H^+}$ | 0.604 | 10 |
| $w_{OH^-}$ | 0.508 | 168 |
| $w_{water}$ | 0.065 | 28 |
| $\lambda_{H^+}$ | 0.758 | 33 |
| $\lambda_{OH^-}$ | 2.300 | 66 |

**Table S5.** Fit RMSD, parameters, and the latter's 90% confidence intervals (in percent) for the *case with ten fitting parameters:* eight reorganization free energies, one for each of the eight elementary steps in the mechanism (four through $H^+$ and four through $OH^-$), and two work terms, one each for transporting water and ions to the surface.

| Parameter (RMSD=0.24) | Value (eV) | Percent 90% c.i. |
|---|---|---|
| $w_{ions}$ | 0.400 | 28 |
| $w_{water}$ | -0.158 | 467 |
| $\lambda_{1,H^+}$ | 1.063 | 440 |
| $\lambda_{1,OH^-}$ | 1.592 | 226 |
| $\lambda_{2,H^+}$ | 0.025 | 541 |
| $\lambda_{2,OH^-}$ | 0.139 | 3012 |
| $\lambda_{3,H^+}$ | 1.712 | 1165 |
| $\lambda_{3,OH^-}$ | 2.841 | 1410 |
| $\lambda_{4,H^+}$ | 1.044 | 3012 |
| $\lambda_{4,OH^-}$ | 2.322 | 787 |

**Table S6.** Fit RMSD, parameters, and the latter's 90% confidence intervals (in percent) for the *case with eleven fitting parameters:* eight reorganization free energies, one for each of the eight elementary steps in the mechanism (four through $H^+$ and four through $OH^-$), and three work terms, one each for transporting water, $H^+$, and $OH^-$ to the surface.

| Parameter (RMSD=0.25) | Value (eV) | Percent 90% c.i. |
|---|---|---|
| $w_{H^+}$ | 0.353 | 1383 |
| $w_{OH^-}$ | 0.708 | 1185 |
| $w_{water}$ | -0.062 | 9559 |
| $\lambda_{1,H^+}$ | 0.336 | 2084 |
| $\lambda_{1,OH^-}$ | 2.183 | 1295 |
| $\lambda_{2,H^+}$ | 1.511 | 1192 |
| $\lambda_{2,OH^-}$ | 1.699 | 933 |
| $\lambda_{3,H^+}$ | 1.783 | 426 |
| $\lambda_{3,OH^-}$ | 1.932 | 1589 |
| $\lambda_{4,H^+}$ | 0.033 | 2142 |
| $\lambda_{4,OH^-}$ | 3.000 | 1072 |

## S6. Using the microkinetic model to inform OER kinetics under acidic/neutral/mildly alkaline solution conditions

In the main text, we presented OER polarization curves for Fe-doped β-NiOOH under alkaline pHs: 13.0, 13.3, 13.7, 14.0, 14.3, and 14.7. It could be useful to examine the relationship between the OER current density and applied potential also at acidic/neutral/mildly alkaline pHs. Accordingly, we plot the OER polarization curves at pHs 0, 2, 4, 6, 7, 8, 10, and 12, in Figures S4 and S5, with the former and latter figures using a linear and log scale, respectively, for the current density. These plots are shown for applied potentials between 1.0 and 1.3 V versus the Hg/HgO electrode. Note that we chose higher applied potentials here (as opposed to between ~0.4 and ~0.7 V in the main text), as the OER current density was always negative for the lower applied potentials at these pHs. As explained in the main text, this is because of the high $H^+$ concentration at low pHs, which unsurprisingly causes the reverse reactions to dominate in the OER mechanism. At pHs 0, 2, and 4, a minimum or inflection point can be seen in the OER current density (Figure S4); such features disappear at higher pHs as all reactions in the OER mechanism begin to proceed in the forward direction. Indeed, at pHs 6 through 12, the characteristic downward-bending behavior of the OER current density on a log scale, as in the main text for pHs 13 and above, is observed (Figure S5). We note that oxyhydroxide catalysts are not particularly stable under acidic solution conditions, due to catalyst dissolution.[3–5] It follows that, although the obtained results for acidic/neutral pHs are interesting from the standpoint of understanding the polarization behavior of the OER across the pH spectrum, the results would likely not represent what would be observed in experiments due to significant catalyst dissolution under such conditions. The additional alkaline pH predictions are more useful, given that the catalyst should survive under those conditions.

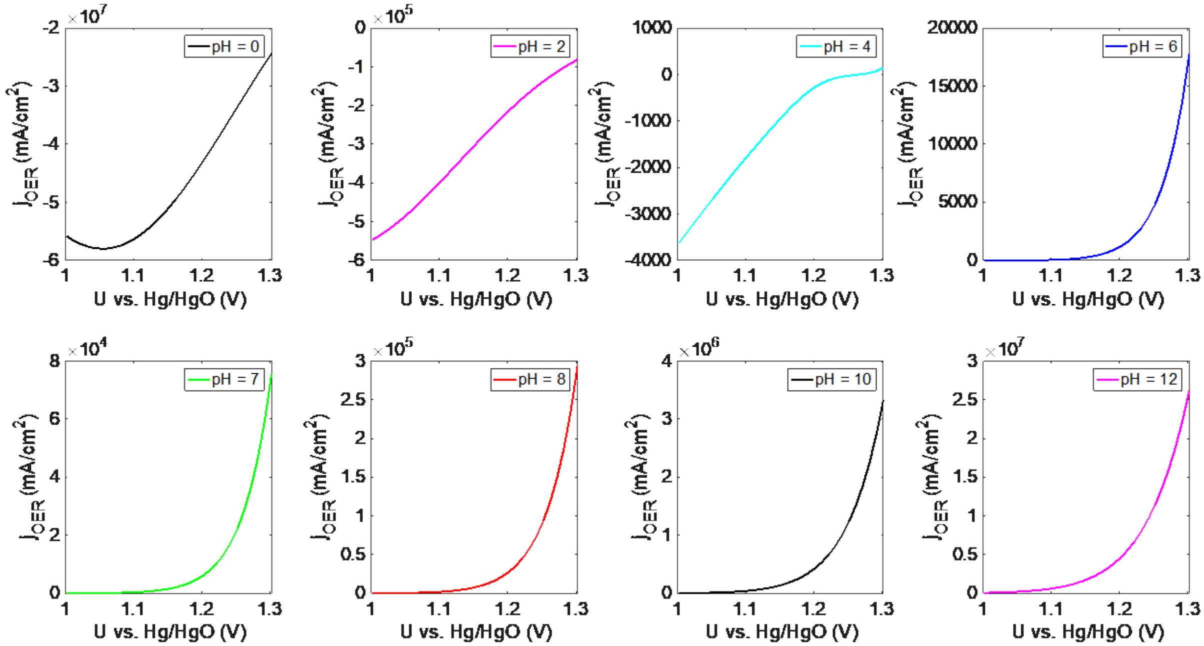

**Figure S4.** OER polarization curves at pHs 0, 2, 4, 6, 7, 8, 10, and 12 for applied potentials between 1.0 and 1.3 V versus the Hg/HgO electrode, with the vertical axes using a linear scale.

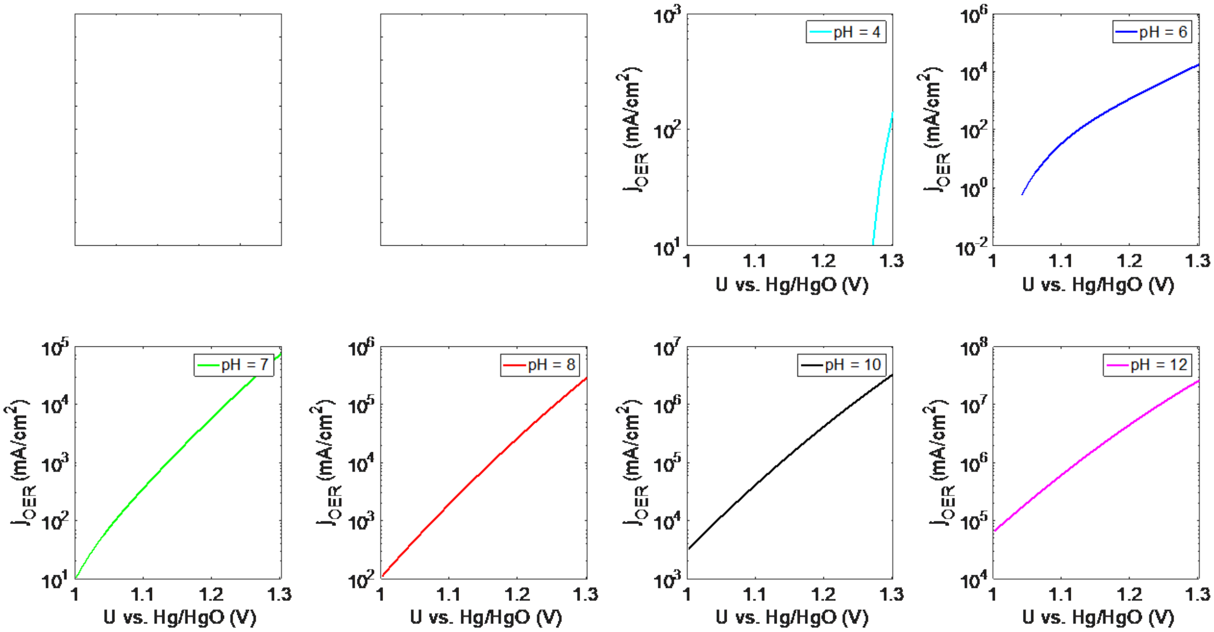

**Figure S5.** OER polarization curves at pHs 0, 2, 4, 6, 7, 8, 10, and 12 for applied potentials between 1.0 and 1.3 V versus the Hg/HgO electrode, with the vertical axes using a log scale. Since the logarithm of a negative number is not a real number, only positive current densities are shown. Accordingly, no data appears for pHs 0 and 2 in these semi-log-scale plots, where each of the predicted current densities are negative. Note also the changes in the vertical scales across the panels.

## S7. Can we conclusively say that the reorganization free energy is lower for reactions involving $H^+$ than for reactions involving $OH^-$?

In the main text, we showed that the observed OER current density on Fe-doped β-NiOOH is primarily attributable to reactions via oxidation of $H_2O$, i.e., via $H^+$, rather than to reactions via $OH^-$, even under alkaline solution conditions. This is a surprising conclusion that merits deeper investigation. Accordingly, we fit the microkinetic model to measured polarization curves while excluding reactions via (a) $OH^-$ and (b) $H^+$. To this end, the forward/backward rate constants for reactions via $OH^-$ and $H^+$ were set to zero, and optimal model parameters, as summarized in Tables S7 and S8, respectively, were determined. We found that the RMSD of the fit deteriorated from 0.26 while including reactions via both $H^+$ and $OH^-$ (see main text or case (i) in section S2 above) to 0.40 while excluding reactions via $OH^-$ to 0.92 while excluding reactions via $H^+$.

The comparisons between the measured and fit polarization curves are presented in Figure S6A and Figure S6B for the cases excluding reactions via $OH^-$ and $H^+$, respectively. The better agreement between the measured and fit polarization curves in panel Figure S6A as compared to Figure S6B is qualitatively consistent with the RMSD being lower in the former case than in the latter case. In both cases, the fit polarization curves are linear, losing their characteristic nonlinear shape, as observed in the main text. Accordingly, the inclusion of both sets of reactions are the key to obtain a good fit of the model to experimental data. Nevertheless, the lower (higher) RMSD for the case excluding reactions via $OH^-$ ($H^+$) indicates that the elementary reactions via protons are more crucial to obtain a good fit of the model with experimental data, also justifying why $\lambda_{H^+} < \lambda_{OH^-}$ in the main text. This is because excluding a particular set of reactions is simply equivalent to the reorganization free energy for that set of reactions being infinity. Accordingly, because reactions via protons are more crucial, it is understandable that their reorganization free energies must be farther from infinity, i.e., lower, as compared to the same quantity for reactions via hydroxide ions.

**Table S7.** Fit RMSD, parameters, and the latter's 90% confidence intervals (in percent) for the *microkinetic model without $OH^-$-based reactions*.

| Parameter (RMSD=0.40) | Value (eV) | Percent 90% c.i. |
|---|---|---|
| $w_{ions}$ | 0.594 | 18 |
| $w_{water}$ | 0.085 | 170 |
| $\lambda_{H^+}$ | 0.258 | 9 |
| $\lambda_{OH^-}$ | 2.472 | $2.2 \times 10^8$ |

**Table S8.** Fit RMSD, parameters, and the latter's 90% confidence intervals (in percent) for the *microkinetic model without $H^+$-based reactions*.

| Parameter (RMSD=0.92) | Value (eV) | Percent 90% c.i. |
|---|---|---|
| $w_{ions}$ | 0.227 | 712 |
| $w_{water}$ | 0.678 | $2.9 \times 10^6$ |
| $\lambda_{H^+}$ | 0.745 | $9.6 \times 10^8$ |
| $\lambda_{OH^-}$ | 2.442 | 131 |

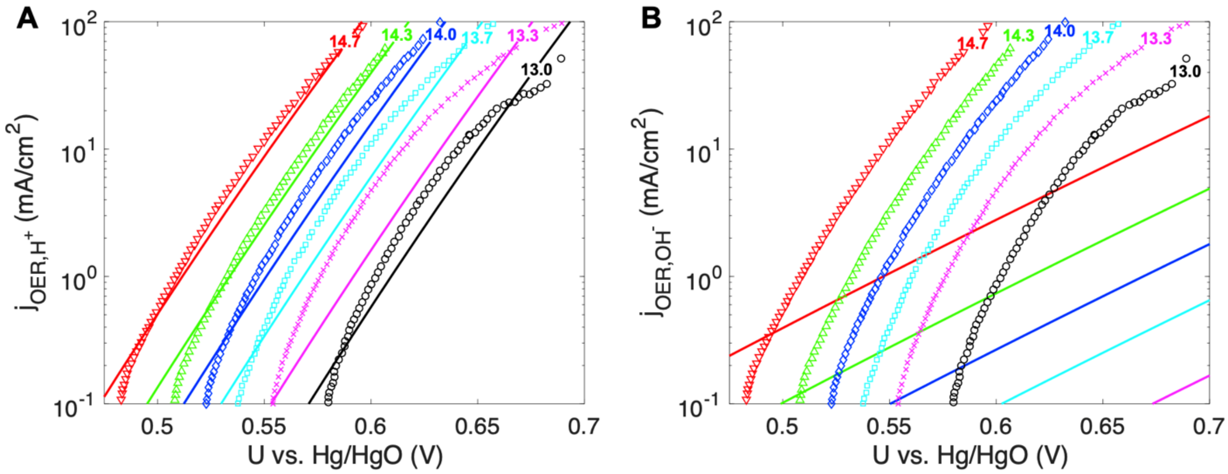

**Figure S6.** Comparison of the fitted and the measured polarization curves (i.e., OER current density vs. applied potential plots) for the microkinetic model without (A) $OH^-$- and (B) $H^+$-based elementary steps included. Experimental data at various pH values are shown using different symbols (13.0 – circles, 13.3 – crosses, 13.7 – squares, 14.0 – diamonds, 14.3 – upward triangles, and 14.7 – downward triangles) and is adapted from the study by Louie and Bell.[2]

## S8. Determining the errors in the charge transfer coefficient and exchange current density obtained from the Tafel analysis

In the main text, the Tafel equation (Eq. (23)) was used to determine the charge transfer coefficient and the exchange current density. Here we re-write the equation for convenience:

$$\eta = \frac{2.303 k_B T}{\alpha e} \log_{10}\left(\frac{j}{j_0}\right) \tag{S7}$$

By expanding the logarithmic term in Eq. (S7), the Tafel equation can also be written as:

$$\eta = \frac{2.303 k_B T}{\alpha e} \log_{10}(j) - \frac{2.303 k_B T}{\alpha e} \log_{10}(j_0) \tag{S8}$$

Based on Eq. (S8), we carried out a linear least-squares fit, $y = mx + c$, as shown in Figure 7 of the main text, where:

$$y = \eta \tag{S9}$$

$$x = \log_{10}(j) \tag{S10}$$

$$m = \frac{2.303 k_B T}{\alpha e} \tag{S11}$$

$$c = -\frac{2.303 k_B T}{\alpha e} \log_{10}(j_0) \tag{S12}$$

Through the fitting procedure using the `regress` function in MATLAB R2017a, we determined the Tafel slope $m$ and the intercept $c$, and their corresponding standard errors $\Delta m$ and $\Delta c$. Subsequently, the charge transfer coefficient was obtained as:

$$\alpha = \frac{2.303 k_B T}{me} \tag{S13}$$

Next, dividing Eq. (S12) by Eq. (S11), we get:

$$\log_{10} j_0 = -\frac{c}{m} \tag{S14}$$

Therefore, the exchange current density can be obtained as:

$$j_0 = 10^{-\frac{c}{m}} \tag{S15}$$

The error in the charge transfer coefficient can be determined by differentiating Eq. (S13):

$$d\alpha = -\frac{2.303 k_B T}{m^2 e} dm \tag{S16}$$

For a small error in the slope, $\Delta m$, one can write the error in the charge transfer coefficient as:

$$|\Delta\alpha| = \frac{2.303 k_B T}{m^2 e} \Delta m \tag{S17}$$

Similarly, the error in the exchange current density can be determined by differentiating Eq. (S15):

$$dj_0 = 10^{-\frac{c}{m}} \times \ln(10) \times \left[\frac{-mdc + cdm}{m^2}\right] \tag{S18}$$

Using Eq. (S14), we get:

$$dj_0 = j_0 \ln(10) \left[\frac{cdm - mdc}{m^2}\right] \tag{S19}$$

For small errors $\Delta m$ and $\Delta c$ in the slope and intercept, respectively, one can write, for the *maximum* error in $j_0$:

$$|\Delta j_0| = j_0 \ln(10) \left[\frac{c\Delta m + m\Delta c}{m^2}\right] \tag{S20}$$

where the minus sign in Eq. (S19) was replaced with a plus sign in Eq. (S20) to obtain the maximum possible error in $j_0$.

Using Eqs. (S17) and (S20), one can estimate the errors in the charge transfer coefficient, $\alpha$, and the exchange current density, $j_0$, respectively. These errors, $|\Delta\alpha|$ and $|\Delta j_0|$, are reported in the main text.

## S9. References

(1) Davis, R. E.; Horvath, G. L.; Tobias, C. W. The Solubility and Diffusion Coefficient of Oxygen in Potassium Hydroxide Solutions. *Electrochim. Acta* **1967**, *12*, 287–297.
(2) Louie, M. W.; Bell, A. T. An Investigation of Thin-Film Ni–Fe Oxide Catalysts for the Electrochemical Evolution of Oxygen. *J. Am. Chem. Soc.* **2013**, *135*, 12329–12337.
(3) Chen, L.; Dong, X.; Wang, Y.; Xia, Y. Separating Hydrogen and Oxygen Evolution in Alkaline Water Electrolysis Using Nickel Hydroxide. *Nat. Commun.* **2016**, *7*, 11741.

(4) Govind Rajan, A.; Martirez, J. M. P.; Carter, E. A. Why Do We Use the Materials and Operating Conditions We Use for Heterogeneous (Photo)Electrochemical Water Splitting? *ACS Catal.* In Press, DOI: 10.1021/acscatal.0c01862.

(5) Li, L.-F.; Li, Y.-F.; Liu, Z.-P. Oxygen Evolution Activity on NiOOH Catalysts: Four-Coordinated Ni Cation as the Active Site and the Hydroperoxide Mechanism. *ACS Catal.* **2020**, *10*, 2581–2590.